Contents lists available at ScienceDirect

Journal of Cartilage & Joint Preservation™

Original Research

VEGF functionalization of suture tape results in decreased graft inflammatory and catabolic response in a rabbit model of ACL reconstruction ☆

Mario Hevesi [a], Carlo A. Paggi [b], Joao F. Crispim [b], Wouter van Genechten [a], Janet M. Denbeigh [a], Nicholas J. Olson [c], Amel Dudakovic [a], Andre J. van Wijnen [a], Aaron J. Krych [a], and Daniel B.F. Saris [a,b,d,*]

[a] Department of Orthopedic Surgery, Mayo Clinic, Rochester, MN, USA
[b] MIRA Institute for Biotechnology and Technical Medicine, University Twente, Enschede, The Netherlands
[c] Department of Pathology, Mayo Clinic, Rochester, MN, USA
[d] Department of Orthopedics, University Medical Center Utrecht, Utrecht University, Utrecht, The Netherlands

ARTICLE INFO

ABSTRACT

Introduction: Improving ligament reconstruction biology may potentially be achieved through capturing autologous circulating factors such as vascular endothelial growth factor (VEGF) using commercially available biomaterials.

Objectives: To evaluate anterior cruciate ligament reconstruction (ACLR) using a VEGF functionalized suture tape in a rabbit model of ACLR with a semitendinosus autograft.

Methods: VEGF-binding peptides were covalently bonded to polyethylene suture tape (ST) to generate functionalized constructs. Forty-six female New Zealand white rabbit ACLs were reconstructed with semitendinosus hamstring autograft ($n = 6$), hamstring + ST ($n = 16$), hamstring + scrambled peptide ST ($n = 17$), and hamstring + VEGF-functionalized ST ($n = 17$). Healing was evaluated at 2 to 4 weeks using PCR, RNA sequencing, micro CT, histology, and biomechanical testing.

Results: All rabbits successfully underwent ACLR, with no adverse events. ACLR with VEGF ST demonstrated significant decreases in inflammatory response (CD14, CD163), catabolism (MMP1, MMP3), and apoptosis (TNFSF10, Caspase-10) markers as compared to nonfunctionalized ST ($P \leq .04$). µCT demonstrated similar bone tunnel mineral density in hamstring + VEGF ST rabbits as compared to hamstring + scrambled ST controls ($P \geq .31$). Histology and biomechanical testing similarly demonstrated no adverse effects of VEGF-based immunomodulation on the tendon grafts.

Conclusions: Using a rabbit model, ACLR performed with VEGF-functionalized suture tape demonstrated significantly decreased markers of inflammation, catabolism, and apoptosis as compared to ACLR with nonfunctionalized suture tape. No adverse effects of functionalization were noted. Future studies should further investigate the utility of functionalized suture tape in ACLR.

Introduction

Anterior cruciate ligament (ACL) injuries are frequent, with considerable morbidity, associated cartilage, and meniscus damage affecting overall joint health, and loss of patient quality of life.[11,13,28] Healing of ACL grafts and the ligamentization process following ACL reconstruction (ACLR) takes time, with recovery lasting 9 to 24 months and beyond.[30] During this period of convalescence, patients have decreased ability to participate in activities of daily living and substantial loss of muscle strength on their operative extremity given their prolonged recovery course.[27] Accordingly, studies have demonstrated that patients have significantly decreased thigh circumference, quadriceps torque, and quadriceps cross sectional area on magnetic resonance imaging (MRI), even at a mean of 49 months following ACLR.[3] Consequently, there is a substantial need for improved biologic healing following ACLR.

Failure of primary ACL grafts occurs in 1% to 10% of patients, with 0 to 4 weeks following reconstruction being a time of particular vulnerability due to early graft necrosis and hypocellularity.[17,23] Subsequently, grafts enter a period of host cellular influx and proliferation, lasting from weeks 4 to 12, leading to graft incorporation and remodeling as well as associated increases in graft mechanical strength.[17] A promising approach to increasing the speed and efficacy of ligament healing may be achieved through capturing autologous, endogenous circulating growth factors on commercially available biomaterials. In particular, Vascular Endothelial Growth Factor (VEGF) has been shown to be intricately involved in healing, inflammation, and revascularization[12,14] and could be used to accelerate and improve ACLR.

While the addition of exogenous compounds can be readily achieved at the time of ACLR, concerns exist regarding appropriate dosing as well as duration of effect given one-time intra-operative administration.[22] An alternative is to employ peptide sequences which reversibly bind and locally concentrate circulating endogenous growth factors.[9] By using such a method, the resultant biologic effect can be sustained and additionally, cellular feedback mechanisms may also better participate in physiologic modulation of growth factor production and, therefore, concentration and availability.[9,31] Given the recent popularization of suture tape (ST) augmentation of constructs to provide mechanical support to ACLR by running in parallel to implanted grafts,[25,29] we believe that these constructs may be an existing, natural target for local peptide binding and concentration.

The purpose of this study was to evaluate ACLR using a VEGF functionalized suture tape construct in a rabbit model of ACLR with a semitendinosus hamstring autograft. In doing so, this study aimed to evaluate the effects of VEGF functionalization on (1) local and systemic adverse effects, (2) markers of healing, inflammation, and catabolism (ie, VEGF, COL1A1), (3) tendon histology, and (4) early graft biomechanics.

Materials and methods

Functionalized FiberWire manufacturing

Vascular endothelial growth factor (VEGF) was chosen for suture tape functionalization given its key role in tissue healing and revascularization. Recent studies have demonstrated that VEGF is more important than other signaling molecules such as fibroblastic growth factor (FGF), in orchestrating healing response, particularly in the setting of ischemic wounds.[7,18] This is of biologic relevance given that early tendon healing following ACLR is dominated by graft necrosis, ischemia, and hypocellularity, particularly during weeks 0 to 4 postoperatively.[1,4,17]

Peptides for capturing VEGF (Protein sequence: KGSWWAPFH) were synthesized using FMOC solid phase methods on a CEM Liberty Blue Peptide Synthesizer (CEM Corporation, Mathews, NC, USA). Peptides were then purified by reversed-phase chromatography using a Jupiter C18 column (Phenomenex, Torrance, CA, USA) and verified by electrospray ionization mass analysis on Agilent 6224 TOF LC/MS instrumentation (Agilent Technologies, Foster City, CA, USA). FiberWire (#2 Diameter AR-7200, Arthrex, Naples, FL, USA) was used as a suture tape for graft internal bracing and also as the chosen biomaterial for functionalization with biopeptides. Sutures were cut into 7 cm pieces and treated with oxygen plasma (Plasma Prep lll, Structure Probe Inc, West Chester, PA, USA) under vacuum conditions for 5 minutes followed by hydrolysis with 1 M sodium hydroxide (#221,465, Sigma Aldrich, St. Louis, MO, USA). Carboxylic acid groups were activated with 0.5 M N–Hydroxysuccinide (NHS, #130,672, Sigma Aldrich, St. Louis, MO, USA) and N'-ethylcarbodiimide hydrochloride (EDC, #25,952–53–8, Creosalus, Louisville, KY, USA) in 0.5 M of 2-ethanesulfonic acid (MES hydrate, #M5287, Sigma Aldrich, St. Louis, MO, USA) buffer for 1 hour. Suture was incubated with 1 mM of VEGF peptide for 30 minutes. Mesh sutures were washed 3 times for 10 minutes with phosphate buffered saline (PBS), sterilized with 1 hour of immersion in 70% ethanol, and stored in sterile containers at 4 °C.

ACL reconstruction

ACL reconstruction was performed following Institutional Animal Care and Use Committee (IACUC) approval and according to ARRIVE guidelines using a standardized, published protocol with 4 month old female New Zealand White rabbits, selected given the species' established translational role in ACL research.[15] In brief, rabbits underwent anesthesia (intramuscular ketamine 35 mg/kg and xylazine 5 mg/kg) with perioperative antibiotic prophylaxis (cefazolin 22 mg/kg) and had the operative extremity shaved, prepped with providone-iodine, and draped in a sterile fashion. A midline incision was made and taken down to the level of the quadriceps and patellar tendon. The medial edge of the quadriceps was then lifted and the semitendinosus exposed and retracted. The distal insertion of the semitendinosus was released sharply and the proximal aspect of the tendon was divided, providing 3 to 4 cm of tendon autograft for subsequent reconstruction. Krakow sutures were placed at both ends of the tendon employing 3–0 FiberWire sutures and the tendon was placed into PBS to prevent desiccation during graft tunnel preparation. A medial parapatellar arthrotomy was then performed. The ACL was identified and excised. Tibial and femoral bone tunnels were created using K-wires to establish anatomic

tunnel trajectory and subsequently over-drilled a 2.5 mm drill. Looped K-wires were passed through the tunnels to allow for passage of the graft. The proximal end of the graft and any associated suture tape was then attached to the cortical crimp construct prior to passing the tendon ± ST through the bone tunnels. The graft was then passed through the tunnels and secured with a second extra-osseous cortical crimp.[15] The knee was then ranged through full range of motion to ensure no restrictions to motion and isometric graft placement. The arthrotomy was re-approximated with interrupted 2–0 Vicryl suture with metal graft fixation (crimps) sutured flush to the periosteum to avoid soft tissue irritation. The subcuticular layer was then closed with interrupted 4–0 Vicryl suture materials under loupe visualization. All New Zealand rabbits obtained for this study were employed and analyzed, without further application of animal-based inclusion / exclusion criteria.

Postoperative care

At the time of procedure end, rabbits were provided a 120 cc subcutaneous bolus of normal saline for postoperative hydration using two 60 cc syringes and a 21 gauge needle. Sustained release buprenorphine (0.12 mg/kg) was provided at the time of surgical closure for postoperative analgesia. Rabbits were placed in Elizabethan collars to protect the surgical site and monitored continuously during initial recovery and then every 12 hours once ambulating. No postoperative immobilization was applied. Any potential complications such as wound infections or weight loss were reviewed with the veterinarian and managed in a way designed to minimize suffering. Rabbits were monitored for veterinarian-vetted humane endpoints including weight loss >20% of body weight, inability to ambulate, and body condition scoring according to local IACUC criteria. Rabbits were euthanized at the planned study endpoints employing phenobarbital euthanasia administered by trained animal care staff.

Molecular characterization of ACLR grafts by polymerase chain reaction analysis

Gene expression was analyzed at the 4 week time point using reverse transcriptase-based real-time quantitative polymerase chain reactions (RT-qPCR). RNA was isolated using a modified Biochain Protocol (Biochain Institute, Newwark, CA, USA). Gene expression for selected gene markers (VEGF, COL1A1, GAPDH) was subsequently quantified using RT-qPCR wherein each reaction was performed with 10 ng/µL of cDNA, QuantiTect SYBR Green PCR kit (Qiagen, Hilden, Germany) and a CFX384 RT-qPCR system (Bio-Rad, Hercules, CA, USA). Transcript levels were quantified and subsequently reported using the $2^{-\Delta\Delta Ct}$ method and normalized to the GAPDH housekeeping gene set at 100.

Comprehensive functionalization characterization using RNA sequencing

RNA sequencing and subsequent bioinformatics analyses were performed for the 4 week time point in collaboration with the Institutional RNA Sequencing and Bioinformatics Core, as previously described in detail.[10,16,19] RNA integrity was assessed using the Agilent Bioanalyzer DNA 1000 chip (Invitrogen, Carlsbad, CA, USA), with samples with an RNA Integrity Number (RIN) greater than 7.5 or DV200 score greater than 50% used for sequencing. Library preparation was performed using the TruSeq RNA library preparation kit (Illumina, San Diego, CA, USA) and polyadenylated mRNAs were selected using oligo dT magnetic beads. Paired-end sequencing reads were generated on the Illumina HiSeq 4000 sequencer. Quality control for concentration and library size distribution was performed using an Agilent Bioanalyzer DNA 1000 chip and Qubit fluorometry (Invitrogen, Carlsbad, CA, USA). Sequence alignment of reads and determination of normalized gene counts were performed using the MAP-RSeq (v.1.2.1) workflow, utilizing TopHat 2.0.6[20] and HTSeq.[2] Normalized read counts were expressed as fragments per kilobasepair per million mapped reads (FPKM).

µCT imaging

µCT imaging (Inveon, Siemens Medical Solutions, Chattanooga, TN) was employed immediately following animal sacrifice and limb harvest at 4 weeks postoperatively in order to asses inner bone tunnel as well as bone tunnel wall bone mineral density (BMD) (Fig. 1). Limbs were scanned employing 360 projections at 80 kV and 500 µA with subsequent imaging analysis (Analyze 12.0, AnalyzeDirect, Stilwell, KS, USA) by independent and blinded Imaging Core personnel.

Histologic tissue characterization

Rabbit knee specimens undergoing histologic analysis were transferred to 10% neutral buffered formalin for preservation immediately following rabbit sacrifice. After 24 hours of fixation, samples were transferred to 70% ethanol for storage prior to embedding. Tissues were embedded into methylmethacrylate and sectioned axially into approximately 25 micron slides using a diamond blade, generating slides for the femoral and tibial bone tunnels as well as the intra-articular portion of the ACL graft. Sections were stained using standard hematoxylin and eosin (H&E) protocols. Subsequently, slides were evaluated by an independent and blinded fellowship trained pathologist employing a standardized histologic scoring system on the basis of graft appearance, graft-bone interface width and tissue nature, presence of inflammatory cells, and graft cellular repopulation (Table 1).
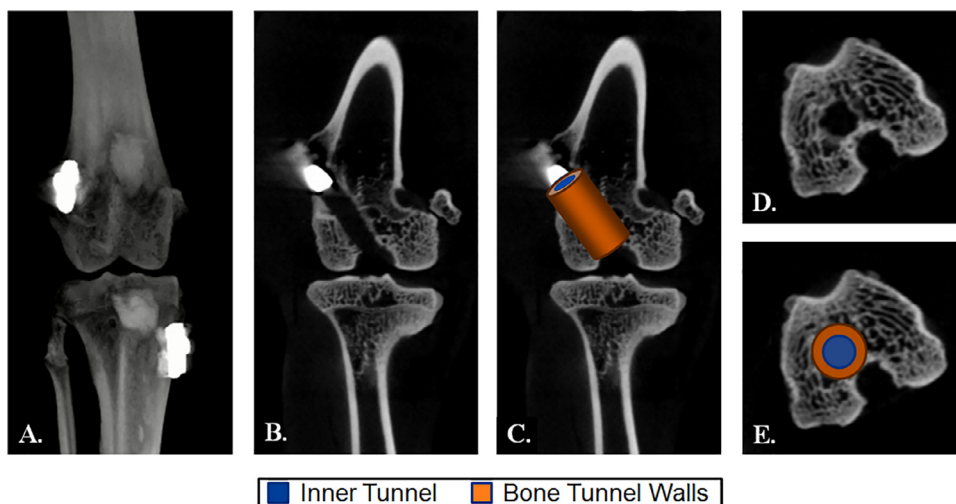
Fig. 1. Assessment of bony tunnel ingrowth at 4 weeks postoperatively. (A) 3D μCT of hamstring + VEGF ST ACLR. (B) Coronal reformat with (C) demonstration of inner tunnel and bone tunnel wall zones where bone mineral density was measured. (D) Axial view of the femur with (E) axial demonstration of measured bone mineral density zones. ACLR, anterior cruciate ligament reconstruction; ST, suture tape; VEGF, vascular endothelial growth factor.

Table 1
Histological ACLR graft grading system.

Criterion:	Score			
	1 Point	2 Points	3 Points	4 Points
Graft appearance	Necrotic	<50% Intact	>50% Intact	Intact
Interface width*	None	Narrow	Average	Profound
Interface tissue*	Fibrous	Fibrocartilage	Sharpey-like	Sharpey Fibers
Inflammatory cells	Predominant	Substantial	Minor	None
Cellular repopulation	None	< 50% graft	> 50% graft	Complete

* Bone-tendon interface. Abbreviation: ACLR, anterior cruciate ligament reconstruction.

Biomechanical testing

Following sacrifice, rabbit lower limbs were dissected, exposing the mid-femur to mid-tibia and sectioning the knee stabilizing ligaments (PCL, MCL, LCL) with the exception of the ACL. The femur and tibia were potted in a 1 inch diameter acrylic tube employing polyurethane resin (Smooth-Cast 300, Smooth-On Inc, Macungie, PA, USA). Specimens were mounted in 45 degrees flexion on a servo-hydraulic mechanical testing frame (MTS 312, MTS Systems, Eden Prairie, MN, USA) with a 200 N capacity load shell. Subsequently, the metal cortical suspensory crimps were cut from the lateral and medial aspect of the femoral and tibial bone tunnels, respectively, thus isolating graft pullout strength to the bone-tendon interface. Load was subsequently applied in an anterior drawer fashion at a rate of 20 mm/min until ACL rupture, with force and displacement recorded at 128 Hz. Peak load (N) to failure and modulus of elasticity was subsequently determined from the force displacement curve.

Safety evaluation

A third party, independent necropsy was performed on $n = 4$ rabbits undergoing ACLR with the VEGF functionalized ST construct to assess for any potential local or systemic adverse effects. Necropsy was performed by institutional, fellowship-trained veterinarians.

Statistics

Measured values were summarized using descriptive statistics including means, standard deviations, and percentages, as appropriate. Ordinal values were compared using Wilcoxon rank-sum testing (Mann-Whitney U) whereas interval values were compared using Student's t-testing. *A priori* power analysis was performed to determine that $n = 3$ samples per group were needed to determine a difference in 1 point per sub-score measured according to the histologic grading system employed. Additionally, for biomechanical endpoints, $n = 4$ rabbits were employed per group to determine an effect size of 3.5 at the 2 week early endpoint and $n = 6$ rabbits were employed to capture an effect size of 2.0 at the final 4 week endpoint with alpha = 0.05 and power = 0.80. In alignment with institutional ethical animal research principles, rabbit samples used for histologic analysis were first analyzed by μCT in order to maximize
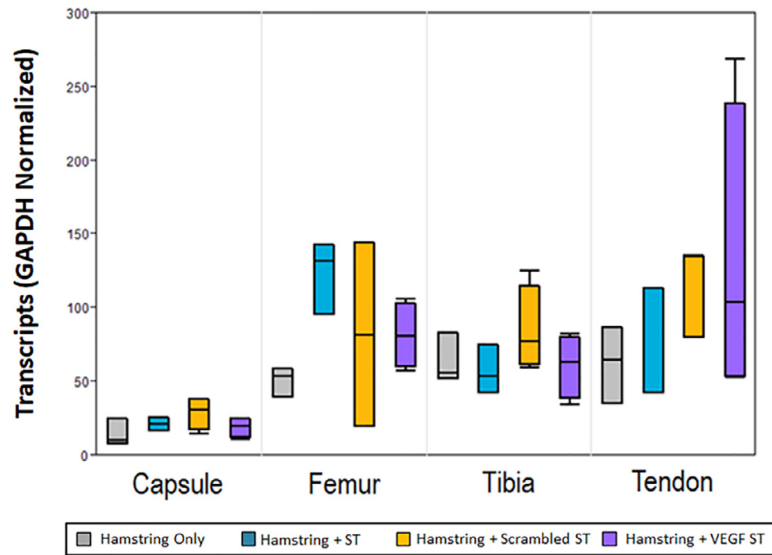
Fig. 2. VEGF expression, as measured by RT-qPCR in the capsule, femur, tibia, and tendon autograft at 4 weeks following ACLR. ACLR, anterior cruciate ligament reconstruction; RT-qPCR, real-time quantitative polymerase chain reactions; ST, suture tape; VEGF, vascular endothelial growth factor.

the use of each sample. Rabbits were randomized using paper randomization to their reconstruction construct (hamstring only, suture tape, suture tape with scrambled peptide, VEGF functionalized suture), with the operating surgeon blinded to the functionalization status of the suture tape being employed intraoperatively in order to minimize the presence of confounders. Animal husbandry staffs were blinded to the reconstruction method used for each animal. Study data were compiled in a standardized database, with unique IDs assigned to each animal and a separate database used to match each animal to suture tape functionalization status at the time of data analysis. Data was available to all study staff and co-authors but was not externally published. P-values $< .05$ were considered significant. Statistics were performed using R Version 3.4.3 (R Core Team, Vienna, Austria) and G*Power 3.1 (G*Power Team, Dusseldorf, Germany).

Results

ACL reconstruction

Forty-six female New Zealand White rabbits successfully underwent ACLR with a semitendinosus hamstring autograft (6 hamstring, 16 hamstring + plain ST, 7 hamstring + scrambled peptide ST, 17 hamstring + VEGF ST). No significant postsurgical events were noted. Rabbits were sacrificed at 4 weeks postoperatively for the PCR, RNA sequencing, histology, and μCT endpoints ($n = 26$ rabbits) and rabbits were sacrificed at 2 ($n = 8$) and 4 weeks ($n = 12$) postoperatively for biomechanical testing. Necropsies were performed by independent, third-party fellowship-trained veterinarians at the 4 week time point for 4 hamstring + VEGF ST rabbits and demonstrated no local or systemic adverse effect of the functionalized suture tape construct.

Molecular characterization with PCR and RNA sequencing

Molecular characterization was begun with limited PCR of the hamstring ($n = 3$), hamstring + plain ST ($n = 3$), hamstring + scrambled ST ($n = 4$) and hamstring + VEGF ST ($n = 4$) tendon grafts at 4 weeks postoperatively to evaluate for a potential effect of suture tape functionalization on tissue VEGF and COL1A1 expression. ACLR performed with hamstring + VEGF ST demonstrated 132.4 ± 101.34 GAPDH normalized transcripts as compared to ACLR with hamstring only (62.4 ± 25.66, $P = .15$), hamstring + ST (66.2 ± 40.4, $P = .17$) and hamstring + scrambled ST (117±31.6, $P = .41$) (Fig. 2). Measured tendon COL1A1 expression was 4383.1 ± 1011.8 for hamstring + VEGF ST as compared to hamstring only (3226.7 ± 1420.9, $P = .26$), hamstring + ST (3386.2 ± 271.0, $P = .16$), and hamstring + scrambled ST (3980.7 ± 1420.9, $P = .66$). Given PCR which suggested potential changes in local gene expression, we then proceeded with comprehensive RNA sequencing of our hamstring + ST and hamstring + VEGF ST samples to more systemically characterize changes brought about by VEGF functionalization.

RNA sequencing analysis demonstrated an overall 2 to 3 fold decrease ($P \leq .04$) in inflammatory response and cellular immunity markers including CD14, CD163, and PI3Ks in the hamstring + VEGF ST group as compared to the hamstring + ST group (Table 2). In addition, catabolic and apoptosis markers including MMP1, MMP3, and Caspase-10 were decreased 2 to 23 fold in the hamstring + VEGF ST group as compared to hamstring + ST controls ($P \leq .03$, Table 2). Of note, there was no cell marker of

Table 2
Selected RNA sequencing target reads for inflammatory response, cellular immunity, catabolism, and apoptosis.

Marker	Effect	Hamstring + ST (FPKM)	Hamstring + VEGF ST (FPKM)	P-value
Inflammatory response and cellular immunity				
CD14	*Monocytes and macrophages*	10,444.3 ± 3122.0	4677.5 ± 2555.3	**.04**
CD163	*Monocytes and macrophages*	727.7 ± 255.0	218.8 ± 87.2	**.01**
HLA-DRA	*Antigen Presentation**	27,798 ± 7318.2	9401.5 ± 5231.8	**.01**
HLA-DPA1	*Antigen Presentation**	1140.7 ± 190.7	394.3 ± 214.6	**<.01**
HLA-DPB1	*Antigen Presentation**	333.8 ± 95.8	149.8 ± 36.6	**.02**
HLA-DMA	*Antigen Presentation**	3873.8 ± 526.5	1485.5 ± 1026.4	**.02**
PIK3CD	*B/T-cell Regulation, Leukocyte Chemotaxis*	387.6 ± 46.9	120.2 ± 29.7	**<.01**
PIK3CG	*B/T-Cell Regulation, Leukocyte Chemotaxis*	1304.3 ± 445.7	510.3 ± 228.5	**.03**
TNFSF13B	*B-cell activation*	1978.0 ± 555.2	630.5 ± 299.8	**<.01**
Catabolism and apoptosis				
MMP1	*ECM breakdown*	2,4711.7 ± 3616.7	5072.8 ± 5044.1	**<.01**
MMP3	*ECM BREAKDOWN*	11,257.5 ± 4860.0	480.2 ± 342.6	**<.01**
Caspase-10	*Apoptosis*	272.7 ± 64.9	136.0 ± 59.6	**.03**
TNFSF10	*Apoptosis*	3069.6 ± 666.3	1444.0 ± 515.4	**.01**
TNFRSF1B	*Apoptosis*	1948.7 ± 177.0	901.8 ± 470.2	**.02**
TNFRSF12A	*Apoptosis*	1638.7 ± 524.1	816.5 ± 117.9	**.03**
TNFRSF21	*Apoptosis*	1884.3 ± 354.8	824.5 ± 385.4	**.01**

All factors surpass a minimum criterion of 2-fold up/downregulation (0.5 < Fold Change [FC] < 2.0).
P-values < 0.05 marked in bold.
Abbreviations: ECM, extracellular matrix; FPKM, fragments per kilobase million reads; TNF, tumor necrosis factor; WBC, white blood cell.
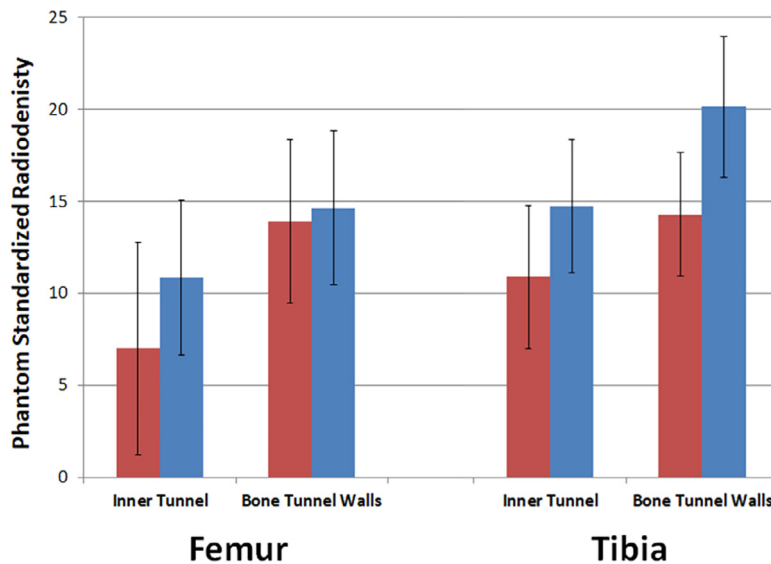 * B-Lymphocytes, Dendritic cells, Macrophages.

Fig. 3. Bone mineral density, as measured by phantom standardized radiolucency for the femur and tibia inner bone tunnels and bone tunnel walls. Hamstring + scrambled ST noted in red; Hamstring + VEGF ST noted in blue. VEGF, vascular endothelial growth factor.

inflammatory response, cellular immunity, or catabolism/apoptosis which was enriched significantly in the hamstring + VEGF ST group.

μCT analysis

μCT was performed immediately following rabbit sacrifice in hamstring + scrambled ST ($n = 3$) and hamstring + VEGF ST ($n = 3$) rabbits. Bone mineral density was found to be statistically similar for the inner tunnels as well as the bone tunnel walls at the 4 week time point for both the femur and tibia ($P \geq .31$, Fig. 3).

Table 3

Histologic ACLR graft grading for the four ACLR reconstruction groups.

Criterion:	Hamstring	Hamstring + ST	Hamstring + scrambled ST	Hamstring + VEGF ST	P-value
Graft appearance	1.2 ± 0.7	1.7 ± 0.7	1.4 ± 0.5	1.5 ± 0.7	.15
Interface width	3.0 ± 1.0	2.3 ± 0.7	3.1 ± 1.0	2.3 ± 1.2	**.02**
Interface tissue	1.7 ± 1.1	2.1 ± 0.8	2.1 ± 1.2	2.6 ± 1.3	.06
Inflammatory cells	2.9 ± 0.3	2.4 ± 0.6	2.6 ± 0.5	2.2 ± 0.7	**<.01**
Cellular repopulation	2.2 ± 0.7	2.6 ± 0.7	2.6 ± 0.8	2.4 ± 0.7	.48
Total score:	10.9 ± 1.9	11.0 ± 1.6	11.7 ± 2.2	11.0 ± 1.7	.77

Abbreviations: ST, suture tape; VEGF, vascular endothelial growth factor.
P-values < 0.05 marked in bold.

Table 4

Biomechanical testing for hamstring + ST and hamstring + VEGF ST peak load and modulus of elasticity.

	Hamstring + ST	Hamstring + VEGF ST	P-value
Peak load at failure (N)			
Week 2	28.53 ± 0.99	34.95 ± 24.22	.74
Week 4	34.75 ± 9.20	41.62 ± 12.56	.30
Modulus of elasticity (N/m^2)			
Week 2	11.73 ± 7.19	10.96 ± 6.00	.89
Week 4	14.84 ± 7.29	13.83 ± 7.73	.82

Abbreviations: ST, suture tape; VEGF, vascular endothelial growth factor.

Histologic tissue characterization

Histologic tissue scoring for graft appearance, interface width and tissue quality, inflammatory cell presence, and cellular repopulation at 4 weeks status post ACLR was performed for the hamstring only ($n = 3$), hamstring + ST ($n = 3$), hamstring + scrambled ST ($n = 3$), and hamstring + VEGF ST ($n = 3$) groups by an independent and blinded fellowship-trained pathologist (Table 3). The 4 ACLR groups were found to demonstrate similar total ACLR graft score, with no adverse histologic reactions noted. However, significant differences were noted between the groups in the Interface Width ($P = .02$) and Inflammatory Cell ($P < .01$) sub-scores. In particular, the interface width of hamstring + scrambled ST was found to be higher than that of hamstring + ST ($P = .01$) and hamstring + VEGF ST ($P = .04$),

Of particular note, inflammatory cell presence also demonstrated a significant overall difference between groups ($P < .01$). Inflammatory cell presence was similar between the 3 ST-containing constructs (plain ST, scrambled ST, VEGF ST, $P \geq .10$) but pairwise comparisons demonstrated that the hamstring only group had substantially higher inflammatory cell scores (fewer inflammatory cells) than hamstring + ST ($P < .01$) and hamstring + VEGF ($P < .01$), suggesting increased overall inflammatory cell presence in the setting of suture tape constructs.

Biomechanical testing

Biomechanical testing was performed at 2 weeks ($n = 8$) and 4 weeks ($n = 12$) to determine pullout strength of the grafts in the bone tunnels (Table 4). Peak load to failure ($P \geq .30$) as well as modulus of elasticity ($P \geq .82$) were found to be statistically similar between the hamstring + ST and hamstring + VEGF ST groups, with peak load and modulus of elasticity measures increasing between the 2 and 4 week time points, as expected with ongoing healing.

Discussion

The main finding of this study is that ACLR with a VEGF functionalized ST was safe and resulted in significant reductions in markers of inflammatory response and catabolism. Furthermore, overall tendon histology and early biomechanics remained statistically similar to ACLR with an internal ST brace, which is increasingly used in current clinical practice.[25,26]

Recently, attention has been turned to the relatively high rupture rates (10%) following primary ACLR, leading to growing consideration of delaying return to sport following ACLR to 2 years and beyond given the extended period needed for graft maturation, return of joint homeostasis, and re-establishment of lower limb functional symmetry.[6,24] Given how common ACL injury is and the extended period of time needed for graft healing and recovery, ACLR is a natural target for biologic augmentation.

VEGF has been described to have profound anti-inflammatory as well as anergic immune effects,[12,14] which are consistent with the substantial decrease in inflammatory and immune signaling observed in the present study during RNA sequencing. This is of importance given the overall detrimental effects of inflammation on tissue healing, maturation, and overall joint health. In this study, scrambled amino acid treatment of suture tape without functionalization was observed to lead to widened, nonphysiologic scarring. In contrast, VEGF functionalized constructs maintained physiologic appearing interfaces, as seen with standard hamstring-only and hamstring + ST healing. Our findings are also supported by previous literature regarding the positive effects of immunomodulation.

Blomgren et al demonstrated that systemic immunosuppression with corticosteroids increased tendon peak force and stiffness by 39% to 58% in an Achilles model of healing, further highlighting the potential role for immune modulation in tendon and ligament repair.[5] However, we believe that immunomodulation is better achieved through local delivery methods as opposed to systemic treatment in order to provide clinically relevant factor concentrations while avoiding side effects of systemic administration.

Functionalization of suture tape in this study was accomplished by covalently bonding a 9 amino acid sequence to polyester jacketed ultra-high molecular weight polyethylene suture, which is already commonly used in the form of an internal brace at the time of ACLR in clinical practice.[26] By using this methodology, autologous circulating VEGF is reversibly bound to the suture tape which runs alongside the hamstring allograft, providing local enrichment of VEGF concentration in a sustained manner.[8,9] This approach is also attractive in that the longitudinal nature of the suture tape from femoral bone tunnel to intra-articular space to tibial bone tunnel has the potential for future poly-functionalization, with differing growth factors used along the intra- and extra-articular portions of the graft.

Regarding our histologic outcomes, overall comparable histologic total graft grading scores were found between functionalized suture tape and the hamstring only group, which models historic ACLR, as well as the hamstring + plain ST group, which is analogous to modern techniques of ACLR with suture tape augmentation.[26] Furthermore, no local or systemic adverse reactions were noted, including the confirmed absence of functionalization-related synovitis during histologic analysis. This is of substantial importance given previous, now historic methods of ACLR with exogenous materials such as carbon fiber, dacron ligament, and Kennedy ligaments were removed from the market in part due to foreign body reactions.[21] Regarding the increased presence of inflammatory cells seen across all ST constructs, this did not significantly vary between plain ST, scrambled ST, and functionalized ST. Additionally, suture tape has an established track record of clinical use in the knee, a reason leading to its selection for this study. Overall, we are reassured that no new changes in inflammatory cell presence were brought about by suture tape functionalization and it will remain important to continue to look for and characterize any cellular response to ST in future studies.

With regards to our µCT analysis, no substantial difference was noted in BMD between the hamstring + VEGF ST and control group, with an overall trend toward increased femoral and tibial BMD values for the VEGF functionalized construct in all comparisons made. Similarly, mechanical pullout strength was found to be statistically similar between VEGF functionalized suture tape and nonfunctionalized suture tape controls. These findings provide further support that functionalization provides clear molecular immunologic and inflammatory modulation while still allowing for ingrowth and remodeling of the suture graft, which is mediated by an influx of host cells into the graft as well as bone-graft interface. Of note, boney ingrowth becomes particularly pronounced at weeks 4 to 12 and beyond, highlighting the utility of future mid- and longer term studies in elucidating bone tunnel healing and pullout strength.

Our study is not without important limitations. First, the present study represents an in vivo proof of concept for suture tape functionalization in a rabbit model. Given the novel nature of the study, sample sizes for analyses including those used for preliminary VEGF PCR analysis were limited in a way that best justified compassionate animal care and use standards for testing new biomaterials. Having established the standard deviation of our observed results, additional experiments can be now carried out with a priori power analysis to best inform sample size. Second, although clear molecular downregulation of inflammatory and catabolic responses were observed in this rabbit study, the translational efficacy of such treatment in humans and its effect on ACL graft failure remains yet to be elucidated. Finally, further, long-term studies are needed to characterize the effect of VEGF functionalization on graft remodeling as well as strength and function at maturity.

Conclusions

Using a rabbit model, ACLR performed with VEGF-functionalized suture tape demonstrated significantly decreased markers of inflammation, catabolism, and apoptosis as compared to ACLR with nonfunctionalized suture tape. No adverse effects of functionalization were noted. Future studies should further investigate the utility of functionalized suture tape in ACLR.

Declaration of competing interest

The authors declare that they have no known competing financial interests or personal relationships that could have appeared to influence the work reported in this paper.

Funding

Author contribution

MH: Study conception/design, data acquisition/interpretation, article drafting, final approval,
CAP: Study conception/design, data acquisition/interpretation, article drafting, final approval,
JFC: Study conception/design, data acquisition/interpretation, article drafting, final approval,
WvG: Study conception/design, data acquisition/interpretation, article drafting, final approval,
JMD: Study conception/design, data acquisition/interpretation, article drafting, final approval,

NJO: Study conception, data acquisition, article drafting and final approval

AD: Study conception, data acquisition/interpretation, article drafting/final approval

AJvW: Study design, data interpretation, article drafting, and final approval.

AJK: Study conception/design, data interpretation, article drafting, and final approval.

DBFS: Study conception/design, data interpretation, article drafting, and final approval.

References

1. Amiel D, Kleiner JB, Akeson WH. The natural history of the anterior cruciate ligament autograft of patellar tendon origin. *Am J Sports Med*. 1986;14(6):449–462.
2. Anders S, Pyl PT, Huber W. HTSeq—a Python framework to work with high-throughput sequencing data. *Bioinformatics*. 2014;31(2):166–169.
3. Arangio GA, Chen C, Kalady M, Reed 3rd JF. Thigh muscle size and strength after anterior cruciate ligament reconstruction and rehabilitation. *J Orthop Sports Phys Ther*. 1997;26(5):238–243.
4. Arnoczky SP, Tarvin GB, Marshall JL. Anterior cruciate ligament replacement using patellar tendon. An evaluation of graft revascularization in the dog. *J Bone Joint Surg Am*. 1982;64(2):217–224.
5. Blomgran P, Hammerman M, Aspenberg P. Systemic corticosteroids improve tendon healing when given after the early inflammatory phase. *Sci Rep*. 2017;7(1):12468.
6. Capin JJ, Khandha A, Zarzycki R, Manal K, Buchanan TS, Snyder-Mackler L. Gait mechanics and second ACL rupture: implications for delaying return-to-sport. *J Orthop Res*. 2017;35(9):1894–1901.
7. Corral CJ, Siddiqui A, Wu L, Farrell CL, Lyons D, Mustoe TA. Vascular endothelial growth factor is more important than basic fibroblastic growth factor during ischemic wound healing. Arch Surg. 1999;134(2):200–205.
8. Crispim J, Fernandes HAM, Fu SC, Lee YW, Jonkheijm P, Saris DBF. TGF-β1 activation in human hamstring cells through growth factor binding peptides on polycaprolactone surfaces. *Acta Biomater*. 2017;53:165–178.
9. Crispim JF, Fu SC, Lee YW, et al. Bioactive tape with BMP-2 binding peptides captures endogenous growth factors and accelerates healing after anterior cruciate ligament reconstruction. *Am J Sports Med*. 2018;46(12):2905–2914.
10. Dudakovic A, Camilleri E, Riester SM, et al. High-resolution molecular validation of self-renewal and spontaneous differentiation in clinical-grade adipose-tissue derived human mesenchymal stem cells. *J. Cell. Biochem.*. 2014;115(10):1816–1828.
11. Filbay SR, Culvenor AG, Ackerman IN, Russell TG, Crossley KM. Quality of life in anterior cruciate ligament-deficient individuals: a systematic review and meta-analysis. *Br J Sports Med*. 2015;49(16):1033–1041.
12. Grau GER, Thompson MB, Murphy CR. VEGF: inflammatory paradoxes. *Pathog Glob Health*. 2015;109(6):253–254.
13. Hagmeijer MH, Hevesi M, Desai VS, et al. Secondary meniscal tears in patients with anterior cruciate ligament injury: relationship among operative management, osteoarthritis, and arthroplasty at 18-year mean follow-up. *Am J Sports Med*. 2019;47(7):1583–1590.
14. Hegde PS, Wallin JJ, Mancao C. Predictive markers of anti-VEGF and emerging role of angiogenesis inhibitors as immunotherapeutics. *Semin Cancer Biol*. 2018;52(Pt 2):117–124.
15. Hevesi M, Crispim JF, Paggi CA, et al. A versatile protocol for studying anterior cruciate ligament reconstruction in a rabbit model. *Tissue Eng Part C Methods*. 2019;25(4):191–196.
16. Hevesi M, Paradise CR, Paggi CA, et al. Defining the baseline transcriptional fingerprint of rabbit hamstring autograft. *Gene Rep*. 2019;15.
17. Janssen RPA, Scheffler SU. Intra-articular remodelling of hamstring tendon grafts after anterior cruciate ligament reconstruction. *Knee Surg Sports Traumatol Arthrosc*. 2014;22(9):2102–2108.
18. Johnson KE, Wilgus TA. Vascular endothelial growth factor and angiogenesis in the regulation of cutaneous wound repair. *Adv Wound Care (New Rochelle)*. 2014;3(10):647–661.
19. Kalari KR, Nair AA, Bhavsar JD, et al. MAP-RSeq: Mayo Analysis Pipeline for RNA sequencing. *BMC Bioinformatics*. 2014;15(1):224.
20. Kim D, Pertea G, Trapnell C, Pimentel H, Kelley R, Salzberg SL. TopHat2: accurate alignment of transcriptomes in the presence of insertions, deletions and gene fusions. *Genome Biol.*. 2013;14(4):R36.
21. Legnani C, Ventura A, Terzaghi C, Borgo E, Albisetti W. Anterior cruciate ligament reconstruction with synthetic grafts. A review of literature. *Int Orthop*. 2010;34(4):465–471.
22. Looney AM, Leider JD, Horn AR, Bodendorfer BM. Bioaugmentation in the surgical treatment of anterior cruciate ligament injuries: a review of current concepts and emerging techniques. *SAGE Open Med*. 2020;8 2050312120921057-2050312120921057.
23. Ménétrey J, Duthon VB, Laumonier T, Fritschy D. Biological failure" of the anterior cruciate ligament graft. *Knee Surg Sports Traumatol Arthrosc*. 2008;16(3):224–231.
24. Nagelli CV, Hewett TE. Should return to sport be delayed until 2 years after anterior cruciate ligament reconstruction? Biological and functional considerations. *Sports Med*. 2017;47(2):221–232.
25. Smith PA, Bradley JP, Konicek J, Bley JA, Wijdicks CA. Independent suture tape internal brace reinforcement of bone-patellar tendon-bone allografts: biomechanical assessment in a full-ACL reconstruction laboratory model. *J Knee Surg*. 2019.
26. Smith PA, Stannard JP, Bozynski CC, Kuroki K, Cook CR, Cook JL. Patellar bone-tendon-bone autografts versus quadriceps tendon allograft with synthetic augmentation in a canine model. *J Knee Surg*. 2020;33(12):1256–1266.
27. Thomas AC, Villwock M, Wojtys EM, Palmieri-Smith RM. Lower extremity muscle strength after anterior cruciate ligament injury and reconstruction. *J Athl Train*. 2013;48(5):610–620.
28. Webster KE, Hewett TE. Meta-analysis of meta-analyses of anterior cruciate ligament injury reduction training programs. *J Orthop Res*. 2018;36(10):2696–2708.
29. Wilson WT, Hopper GP, Byrne PA, MacKay GM. Anterior cruciate ligament repair with internal brace ligament augmentation. *Surg Technol Int*. 2016;29:273–278.
30. Zaffagnini S, Grassi A, Serra M, Marcacci M. Return to sport after ACL reconstruction: how, when and why? A narrative review of current evidence. *Joints*. 2015;3(1):25–30.
31. Zara JN, Siu RK, Zhang X, et al. High doses of bone morphogenetic protein 2 induce structurally abnormal bone and inflammation in vivo. *Tissue Eng Part A*. 2011;17(9–10):1389–1399.